Proceedings of IMECE2007
2007 ASME International Mechanical Engineering Congress and Exposition
November 11-15, 2007, Seattle, Washington, USA

IMECE2007-43921

COMPUTERIZED PLANNING OF MULTI-PROBE CRYOSURGICAL TREATMENT FOR TUMOR WITH COMPLEX GEOMETRY

Zhong-Shan Deng [1], Jing Liu [1, 2]

1. Cryogenics Laboratory, P. O. Box 2711, Technical Institute of Physics and Chemistry, Chinese Academy of Sciences, Beijing 100080, China

2. Department of Biomedical Engineering, School of Medicine, Tsinghua University, Beijing 100084, China

ABSTRACT

To perform a cryosurgical procedure successfully, it is important to carefully design the optimal freezing parameters (such as the number of cryoprobes, the locations, the insertion paths and depths of cryoprobes) before cryosurgery. Failure to do so accurately could lead to either insufficient or excessive freezing. Due to the irregularly shaped tumors commonly encountered in clinics, multiple cryoprobes are often needed, which makes the parameter optimization rather difficult. Computerized planning tools would help to alleviate this difficulty. In this study, a three-dimensional cryosurgery planning tool is developed, based on the numerical algorithm presented in our recent works. This tool is developed with general purpose and applicable for the treatment planning of tumor with complex geometry. For demonstration purposes, several examples for typical cryosurgery cases using multiple cryoprobes are given and interpreted.

INTRODUCTION

Cryosurgery, the controlled destruction of undesirable tissues by local freezing, has been used as a minimally invasive technique for treatment of many types of tumors [1]. The basic objective of cryosurgery is to destroy the cells or tissue within a closely defined region and allow complete recovery of all tissue outside this region. Practically, this translates to encompassing the whole of the tumor volume with irregular shape and none of the healthy tissue by a critical isotherm [2]. Unfortunately, the noninvasive, real-time monitoring of three-dimensional isotherm surface of this critical temperature within the tissue during cryosurgical procedures has remained a challenge. Consequently, cryosurgical treatment becomes an art held by the cryosurgeon, based on the surgeon’s own experience.

In fact, the temperature distribution of tissue around a cryoprobe is predictable and can be modeled using computer simulation [3-5]. Similar to the treatment planning strategies used for radiation therapy, it is possible to determine optimal cryoprobe placements to inflict lethal freezing injury to tumor while sparing the normal tissues in the vicinity of tumor. As is well known, the outcome of cryosurgery depends on various factors, such as the number of cryoprobes used, cryoprobe placements and cryoprobe thermal protocol. To attain optimal outcome, the cryoprobe placements and the freezing procedures used have to take account of the corresponding lethal region by cryogenic temperatures.

In this work, we extended the numerical algorithm presented in our recent works to the more difficult case of in vivo application, and then developed a three-dimensional cryosurgery planning tool. It is more difficult due to the irregularly shaped tumors, which complicates the setting of tumor domain. The purpose of this work was to optimize the number of cryoprobes used and their positions in irregularly shaped tumors before actual cryosurgery. This planning tool also provides a means of assessing effectiveness of cryosurgical treatment.

MATHEMATICAL MODEL AND ALGORITHM

The process of treatment planning is based on a sequence of bioheat transfer simulations of the cryosurgical procedure. The numerical algorithm used for the current cryosurgical planning tool has been developed by Deng and Liu [6], and is presented here briefly. Due to the freezing of cryoprobes, the whole tissue domain consists of unfrozen tissue and frozen tissue domains. It is customary to model the heat transfer in unfrozen tissue (in the presence blood perfusion) by the classical bioheat equation [7]:

$$C\frac{\partial T(\mathbf{X},t)}{\partial t} = \nabla \cdot k\nabla\left[T(\mathbf{X},t)\right] - \omega_b C_b T(\mathbf{X},t) + Q_m + C_b \omega_b T_a \quad (1)$$

where C, C_b are respectively the heat capacity of biological tissue and blood; $\mathbf{X}$ contains the Cartesian coordinates x, y and z; k is the thermal conductivity of tissue; ω_b is the blood perfusion; T_a is the arterial temperature, and T the tissue temperature; and Q_m is the metabolic heat generation.

For the frozen tissue, due to absence of blood flow and metabolic activities, the heat transfer is controlled by Fourier's law. By introducing effective heat capacity $\tilde{C}$, effective thermal conductivity $\tilde{k}$, effective blood perfusion $\tilde{\omega}_b$, and effective metabolic heat generation $\tilde{Q}_m$, the uniform energy equation for the unfrozen and frozen biological tissues can be written as [6]:

$$\tilde{C}\frac{\partial T}{\partial t} = \nabla \cdot \tilde{k}\nabla T - \tilde{\omega}_b C_b T + \tilde{Q}_m + \tilde{\omega}_b C_b T_a, \quad \mathbf{X} \in \Omega \quad (2)$$

where Ω denotes the analyzed domain. The definitions of the above effective quantities are as follows:

$$\tilde{C}(T) = \begin{cases} C_f, & T < T_{ml} \\ \dfrac{\rho Q_l}{\left(T_{mu} - T_{ml}\right)} + \dfrac{C_f + C_u}{2}, & T_{ml} \le T \le T_{mu} \\ C_u, & T > T_{mu} \end{cases} \quad (3)$$

$$\tilde{k}(T) = \begin{cases} k_f, & T < T_{ml} \\ \left(k_f + k_u\right)/2, & T_{ml} \le T \le T_{mu} \\ k_u, & T > T_{mu} \end{cases} \quad (4)$$

$$\tilde{Q}_m(T) = \begin{cases} 0, & T < T_{ml} \\ 0, & T_{ml} \le T \le T_{mu} \\ Q_m, & T > T_{mu} \end{cases} \quad (5)$$

$$\tilde{\omega}_b(T) = \begin{cases} 0, & T < T_{ml} \\ 0, & T_{ml} \le T \le T_{mu} \\ \omega_b, & T > T_{mu} \end{cases} \quad (6)$$

The tissue domain is prescribed in a rectangular geometry with 5×10×10 cm in the *x*, *y* and *z* directions respectively, in which *x* denotes the tissue depth from the skin surface while *y* and *z* are along the surface. In the calculations, the cylindrical probe is approximated by a cube. The boundary conditions at the probe surface are prescribed respectively according to probe tip and probe shank as:

$$T = T_w \text{ at probe tip}; \quad \partial T/\partial n = 0 \text{ at probe shank} \quad (7)$$

The conditions at the boundaries of cubic calculation domain are defined as follows:

$$-k\frac{\partial T}{\partial x} = h_f\left[T_f - T\right] \text{ at } x = 0; \quad T = T_c \text{ at } x = 0.05\text{ m} \quad (8)$$

$$\partial T/\partial y = 0 \text{ at } y = 0; \quad \partial T/\partial y = 0 \text{ at } y = 0.1\text{ m} \quad (9)$$

$$\partial T/\partial z = 0 \text{ at } z = 0; \quad \partial T/\partial z = 0 \text{ at } z = 0.1\text{ m} \quad (10)$$

where T_c and T_f are the temperatures of body core and surrounding air, respectively; and h_f is the convective heat transfer coefficient between the environment and skin. The initial temperature in tissue is simplified as T_0=37 °C.

A finite difference algorithm developed in our previous study [6] is applied to solve this complex problem with phase change heat transfer in biological tissues. The description and derivation of the algorithm are omitted here for brevity. In calculations, the grid resolution is $\Delta x = \Delta y = \Delta z = 0.001$ m and $\Delta t = 0.1$ s.

Irregularly shaped tumors may require careful considerations for finding the optimal number and positions of the cryoprobes before performing cryosurgery. This can be done when a digitized image of the tumor selected for cryosurgery is available. To begin the optimization process with probes, it is necessary to select an initial configuration. Next, the corresponding bioheat transfer simulation is computed. Then by superimposing the calculated patterns of isotherms on the image of the tumor it can be seen whether with the selected number and placement of cryoprobes all regions of the tumor are lethally frozen. If not, the position of the misplaced cryoprobes can be changed until calculations show that the entire tumor is frozen to lethal temperature.

RESULTS AND DISCUSSION

In the following calculations, the typical tissue properties are applied as given in [6]: $C_b = C_u = 3.6\,\text{MJ/m}^3\cdot°\text{C}$, $C_f = 1.8\,\text{MJ/m}^3\cdot°\text{C}$, $k_f = 2\,\text{W/m}\cdot°\text{C}$, $k_u = 0.5\,\text{W/m}\cdot°\text{C}$, $Q_L = 250\,\text{MJ/m}^3$, $T_a = 37°\text{C}$, $T_{ml} = -8°\text{C}$, $T_{mu} = -1°\text{C}$. The placements of cryoprobes are given in Table 1. The temperature of probe tip is assumed to be constant (T_w= –196°C). For normal and tumor tissues, both the blood perfusion and metabolic rate are very different [6], which are respectively taken as:

$$\omega_b = \begin{cases} 0.0005\,\text{ml/s/ml}, & x,y,z \notin \Omega_t \\ 0.002\,\text{ml/s/ml}, & x,y,z \in \Omega_t \end{cases}$$

$$Q_m = \begin{cases} 4200\,\text{W/m}^3, & x,y,z \notin \Omega_t \\ 42000\,\text{W/m}^3, & x,y,z \in \Omega_t \end{cases}$$

To encompass the whole of a large tissue mass, such as a large tumor, multiple cryoprobes must be used. Whenever multiple probe insertions are used, however, great care must be taken at the design of the optimal number and positions of the cryoprobes before performing cryosurgery because overlapping of the freezing zone will amount to repetitive freezing of these areas with tissue destruction beyond the predetermined zone of coagulation. Figure 1 presents the case of 3 cryoprobes with different depth for treatment of large tumor, in which the surface of ice ball is determined by the isothermal surface of T_{mu}= –1°C (similarly hereinafter for the other calculation examples). The location and size of tumor applied in the calculation is shown in Fig. 1(a), in which the geometrical parameters of the tumor can be easily read. From Fig. 1(c) and Fig. 1(d), it is clearly seen that the ice ball has encompassed the whole tumor with similar shape. It indicates that the placements of cryoprobes used here have been optimal.

Table 1: the optimal placements of cryoprobes

		Domain of probe tip(s)
The case of 3 probes with different depths	Probe 1	0.017 m ≤ x ≤ 0.027 m 0.048 m ≤ y ≤ 0.052 m 0.052 m ≤ z ≤ 0.056 m
	Probe 2	0.016 m ≤ x ≤ 0.026 m 0.043 m ≤ y ≤ 0.047 m 0.043 m ≤ z ≤ 0.047 m
	Probe 3	0.015 m ≤ x ≤ 0.025 m 0.053 m ≤ y ≤ 0.057 m 0.043 m ≤ z ≤ 0.047 m
The case of 2 probes with the same size	Probe 1	0.02 m ≤ x ≤ 0.03 m 0.036 m ≤ y ≤ 0.042 m 0.036 m ≤ z ≤ 0.042 m
	Probe 2	0.015 m ≤ x ≤ 0.025 m 0.052 m ≤ y ≤ 0.058 m 0.058 m ≤ z ≤ 0.064 m
The case of 2 probes with different sizes	Probe 1	0.021 m ≤ x ≤ 0.029 m 0.037 m ≤ y ≤ 0.041 m 0.037 m ≤ z ≤ 0.041 m
	Probe 2	0.015 m ≤ x ≤ 0.025 m 0.052 m ≤ y ≤ 0.058 m 0.058 m ≤ z ≤ 0.064 m

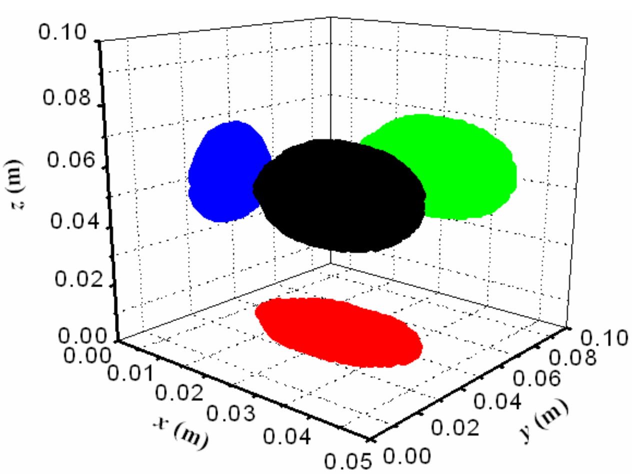

(a) the location and size of tumor

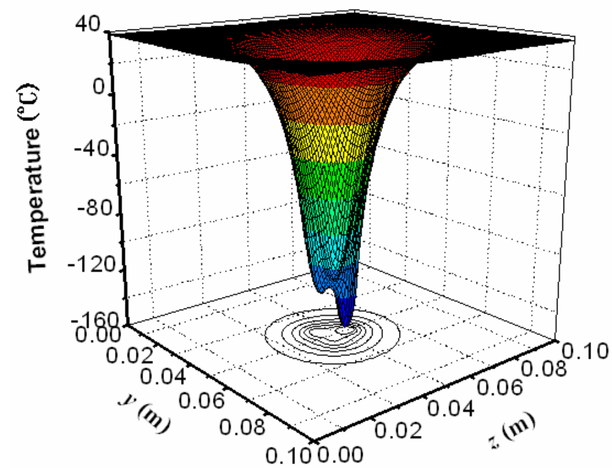

(b) temperature distribution at x=0.027 m (t=1200 s)

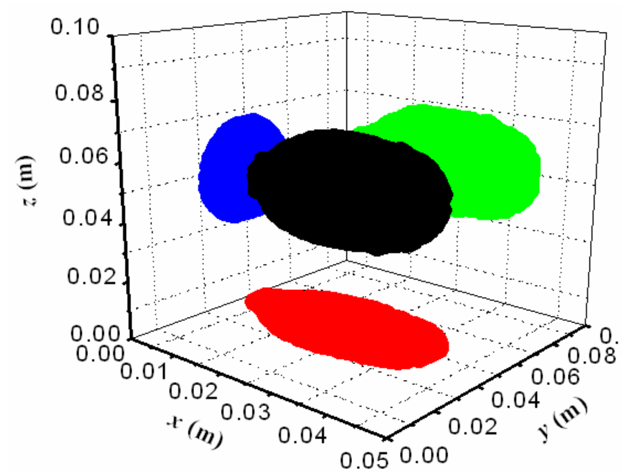

(c) the location and size of ice ball at t=900 s

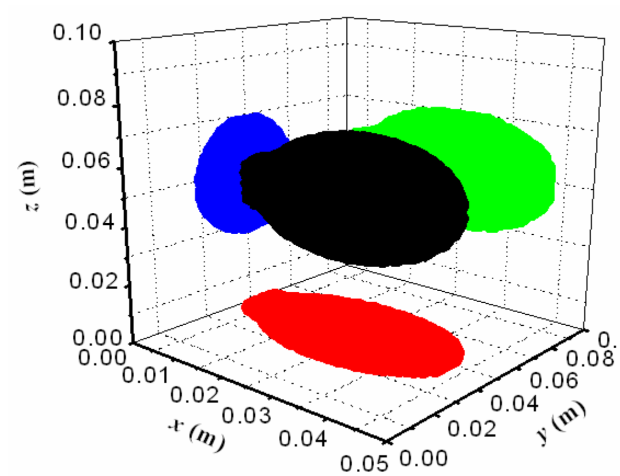

(d) the location and size of ice ball at t=1200 s

Fig. 1. The case of 3 probes with different depths

As is well known, the shape of tumor usually appears as highly irregular. Before performing cryosurgery, irregularly shaped tumors also require careful considerations for finding the optimal number and positions of the cryoprobes. The optimization of cryoprobe placements for highly irregular tumor is shown in Fig. 2 and Fig. 3. The geometrical parameters of the tumors applied in the calculations can be easily read from Fig. 2(a) and Fig. 3(a), respectively. The difference between the tumors in Fig. 2(a) and Fig. 3(a) is that the geometrical shape of the tumor in Fig. 3(a) is more complex. It can be clearly seen from Fig. 2(b) and Fig. 3(b) that the ice ball has encompassed the whole tumor with similar shape. Therefore, the results in Fig. 2(b) and Fig. 3(b) indicate that the placements of cryoprobes given in Table 1 are also optimal.

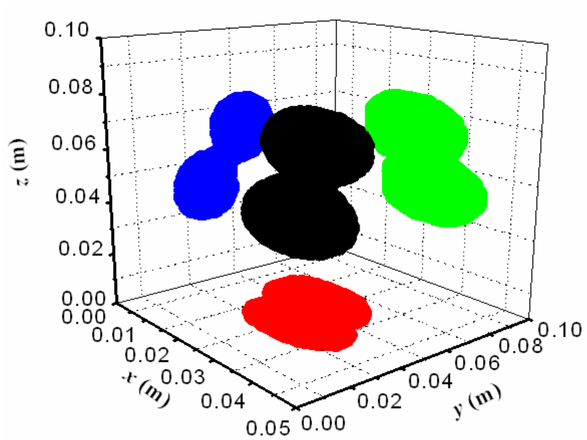

(a) the location and size of tumor

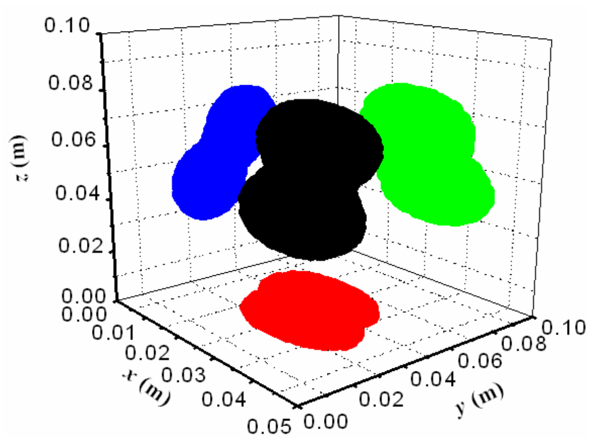

(b) the location and size of ice ball at t=1200 s

Fig. 2. The case of 2 probes with the same size

The above calculations have quantitatively illustrated that the computerized planning tool presented in this article is suitable for the treatment planning of tumor with complex geometry. In addition, this planning tool can also be used to evaluate the rationality of a given treatment protocol. However, it should be pointed out that our present analysis has not included the effect of large blood vessels. This feature will be discussed in our future work.

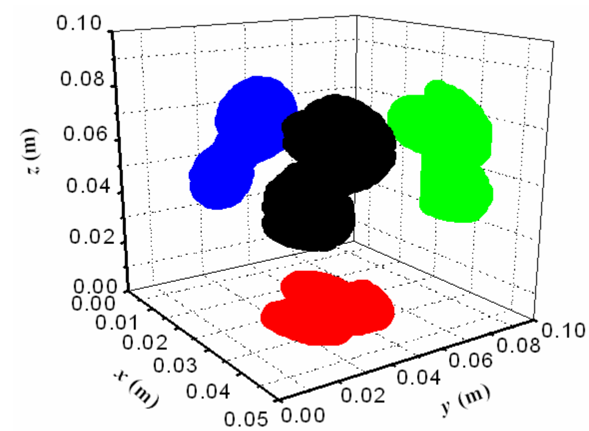

(a) the location and size of tumor

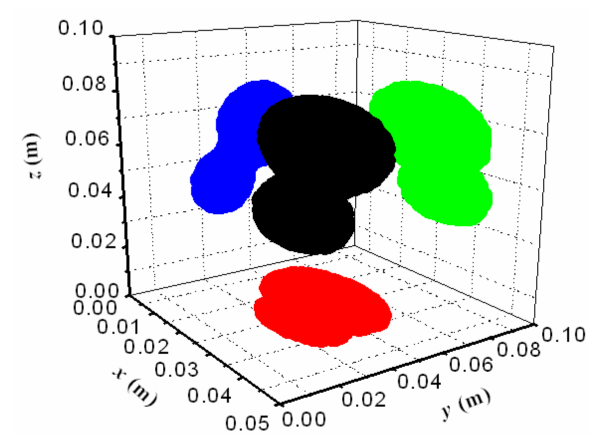

(b) the location and size of ice ball at t=1200 s

Fig. 3. The case of 2 probes with different sizes

CONCLUSIONS

A numerical optimization tool for multiple cryoprobe placements has been presented. Two features of this planning tool were particularly illustrated: (1) optimization of multiple cryoprobes for large tumors, and (2) optimization of cryoprobe placements for high irregularly shaped tumor. In summary, results of this study should be considered in cryosurgical applications for designing an optimal placement of cryoprobes.

NOMENCLATURE

C	Heat capacity (J/m^3·°C)

h_f	Convective heat transfer coefficient (W/m^2·°C)
k	Thermal conductivity (W/m·°C)
Q_l	Latent heat (J/m^3)
Q_m	Metabolic heat generation (W/m^3)
t	Time (s)
T	Temperature (°C)
T_a	Artery temperature (°C)
T_c	Body core temperature (°C)
T_f	Surrounding air temperature (°C)
T_{ml}	Lower phase transition temperature (°C)
T_{mu}	Upper phase transition temperature (°C)
T_w	Temperature at probe tip (°C)
x, y, z	Cartesian coordinate
$\mathbf{X}$	Location
α	Thermal diffusivity of tissue (m^2/s)
β	Parameter taking the value between 0 and 1
ω_b	Blood perfusion (ml/s/ml)
Δ	Step size
Ω	Computation domain

Subscripts

0	Initial value
b	Blood
f	Frozen tissue
u	Unfrozen tissue

ACKNOWLEDGMENTS

This work was partially supported by the National Natural Science Foundation of China (under Grants 50576104 & 50325622) and the Initial Funding for the Gainer of Excellent Doctoral Dissertation of CAS.

REFERENCES

[1] Rubinsky B., 2000, "Cryosurgery," Annual Review of Biomedical Engineering, **2**, pp. 157-187.

[2] Gage A. A., and Baust J., 1998, "Mechanism of tissue injury in cryosurgery," Cryobiology, **37**, pp. 171–186.

[3] Keanini R. G., and Rubinsky B., 1992, "Optimization of multiprobe cryosurgery," ASME Journal of Heat Transfer, **114**, pp. 796-801.

[4] Rewcastle J. C., Sandison G. A., Muldrew K., Saliken J. C., and Donnelly B. J., 2001, "A model for the time dependent three-dimensional thermal distribution within iceballs surrounding multiple cryoprobes," Medical Physics, **28**, pp. 1125-1137.

[5] Sandison G. A., 2002, "Future directions for cryosurgery treatment planning," Urology, **60**, pp. 50-55.

[6] Deng Z. S., and Liu J., 2004, "Numerical simulation on 3-D freezing and heating problems for the combined cryosurgery and hyperthermia therapy," Numerical Heat Transfer, Part A: Applications, **46**, pp. 587-611.

[7] Pennes H. H., 1948, "Analysis of tissue and arterial blood temperatures in the resting human forearm," Journal of Applied Physiology, **1**, pp. 93-122.